

# Photocatalytic C–H Amination of Electron-rich Aromatic Hydrocarbons by Carbon Nitride Photocatalysis

Stefano Mazzanti<sup>+</sup>,<sup>[a]</sup> Yevheniia Markushyna<sup>+</sup>,<sup>[a]</sup> and Oleksandr Savatiev<sup>\*[a]</sup>

Construction of C–N bond is a central process in organic synthesis. Typically, it relies on noble-metal catalysts and prefunctionalized substrates, such as aryl halides. Alternative and more appealing method is a direct C–H amination of hydrocarbons that is based on intrinsic reactivity of the *in situ* generated radical cations, which are more electrophilic compared to their closed-shell precursors. In this work, we employ potassium poly(heptazine imide) (K-PHI), a graphitic carbon

nitride semiconductor, to enable C–H amination of electron rich aromatic hydrocarbons with NH<sub>3</sub> and pyrazole under oxidative conditions. Screening of oxidants, indicate those molecules that are able to accept not only electrons, but also protons, such as O<sub>2</sub>, PhNO<sub>2</sub> and Ph<sub>2</sub>S<sub>2</sub>, mediate the reaction. As such, multisite proton-coupled electron transfer (MS-PCET) from the photo-charged state of K-PHI to the acceptor of electrons and protons is the key element in the studied photocatalytic process.

## Introduction

The ever-growing need for new drug candidates, always more complex, brought industrial companies in cooperation with academic partners for the development of unseen chemical reactivities.<sup>[1]</sup> Cutting-edge science for this purpose relies on organocatalysis,<sup>[2]</sup> electrosynthesis,<sup>[3]</sup> photoelectrocatalysis<sup>[4,5]</sup> and photoredox catalysis.<sup>[6]</sup> The latter one has been by far the most employed in industry and it is widely explored for the synthesis of active pharmaceutical ingredients (APIs).<sup>[7]</sup> The ability to generate open-shell intermediates under visible light provides a new opportunity for developing the most variegated types of chemical functionalization while avoiding undesired side reactions caused by high-energy photons (e.g. UV).<sup>[8,9]</sup>

Cross-couplings are among the most employed methods exploited for the production of APIs.<sup>[10,11]</sup> For this reason, photocatalytic methods are also used for C–N bond formation in the preparation of substituted anilines.<sup>[12]</sup> Thus, a combination of Ni-catalyst and a sensitizer, such as Ir-polypyridyl complex,<sup>[13]</sup> mesoporous graphitic carbon nitrides (mpg-CN),<sup>[14]</sup> ionic carbon nitride (CN-OA-m),<sup>[15]</sup> enable coupling of aryl halides with primary and secondary amines. On the other hand, unsubstituted anilines are accessible *via* dual Ni/carbon nitride

photocatalytic approach employing aryl halides, sodium azide, and triethylamine as a donor of electrons and protons.<sup>[16]</sup> An alternative group of methods is based on the direct coupling of hydrocarbons, employing their intrinsic reactivity, with amines without aromatic substrate prefunctionalization. Thus, [Mes-Acr]<sup>+</sup>/TEMPO system enables the coupling of a broad scope of azoles with electron-rich aromatic hydrocarbons.<sup>[12d]</sup> Wang and König reported hexagonal boron carbon nitride (*h*BCN) as a heterogeneous and reusable photocatalyst and O<sub>2</sub> as electron acceptor to couple electron rich hydrocarbons with azoles, while for preparation of unsubstituted anilines ammonium salts were used.<sup>[17]</sup> Nevertheless, for the preparation of unsubstituted anilines, more appealing would be aqueous ammonia solution as the cheapest NH<sub>3</sub> source.

The mechanistic studies indicate that the role of photocatalysts is to generate a radical cation from the hydrocarbon, which is more susceptible to nucleophilic attack of NH<sub>3</sub> or azole. Therefore, for productive photocatalysis valence band potential of a semiconductor must be more positive than the oxidation potential of the hydrocarbon. This primary requirement for the highly positive potential of the valence band, i.e. +1.88 V vs. SCE, is met in ionic carbon nitrides, such as potassium poly(heptazine imide) (K-PHI).<sup>[18]</sup> The material is obtained under ionothermal conditions by heating nitrogen-rich precursor, such as melamine or 5-aminotetrazole, in eutectic mixture of LiCl/KCl or KCl at 600 °C (see figure S1 for characterization data).<sup>[19]</sup> The material is composed of heptazine units interconnected *via* deprotonated (sp<sup>2</sup>)N atoms, while K<sup>+</sup> ions serve to compensate negative charge (Figure 1a).<sup>[20,21]</sup>

Combination of medium band gap energy (2.7 eV) and valence band potential of +1.88 V vs. SCE is translated into the conduction band potential of –0.82 V vs. SCE, which renders the photogenerated electrons to be only moderately reductive. K-PHI also possesses a unique for graphitic carbon nitrides property to undergo photocharging.<sup>[22]</sup> This property is attributed mainly to the following features: *i*) ionic structure of the material screens charges<sup>[23]</sup> and allows for gradual accumulation of electrons upon irradiation of K-PHI in the presence of

[a] Dr. S. Mazzanti,<sup>+</sup> Dr. Y. Markushyna,<sup>+</sup> Dr. O. Savatiev  
Department of Colloid Chemistry  
Max Planck Institute of Colloids and Interfaces  
Am Mühlenberg 1  
14476 Potsdam (Germany)  
E-mail: oleksandr.savatieiev@mpikg.mpg.de

[<sup>+</sup>] These authors contributed equally.

Supporting information for this article is available on the WWW under <https://doi.org/10.1002/cctc.202201388>

This publication is part of a Special Collection on "Photocatalytic Synthesis". Please check the ChemCatChem homepage for more articles in the collection.

© 2023 The Authors. ChemCatChem published by Wiley-VCH GmbH. This is an open access article under the terms of the Creative Commons Attribution Non-Commercial License, which permits use, distribution and reproduction in any medium, provided the original work is properly cited and is not used for commercial purposes.

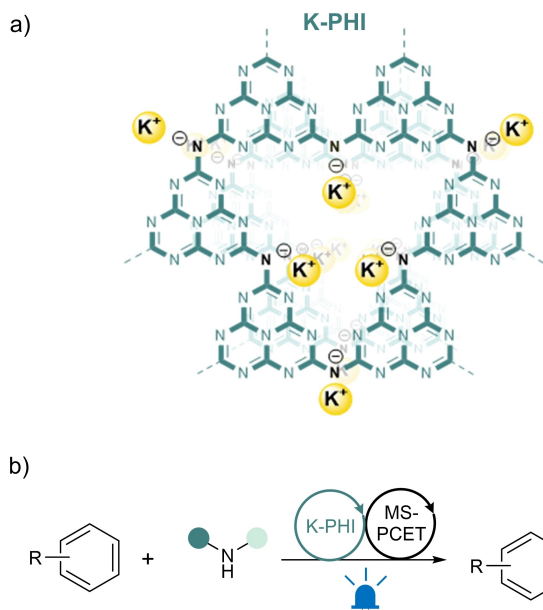


**Figure 1.** Concept and reaction design. a) Potassium poly(heptazine imide) (K-PHI) structure. b) C–H amination of aromatic hydrocarbons mediated by K-PHI via MS-PCET proposed in this work.

electron donors; *ii*) highly crystalline domains favor the delocalization of electrons over the aromatic structure; *iii*) a highly positive potential of the valence band promotes easy electron uptake from substrates; *iv*) the microporous structure, which is shown in TEM image in Figure S2, allows for the storage of counterbalancing protons (or other cations) inside the nanoparticle in addition to the surface.<sup>[24,21,25]</sup> Taken all together, poly(heptazine imides) are a unique heterogeneous platform for multisite-proton coupled electron transfer processes (MS-PCET).<sup>[26]</sup> By combining K-PHI, an electron donor and light, it is possible to mimic natural photosynthesis and transform endergonic reactions that are based on electron transfer (ET) into spontaneous processes that proceed *via* proton-coupled electron transfer (PCET, Calvin cycle).<sup>[27]</sup> In the context of aromatic hydrocarbons C–H amination with aqueous ammonia, MS-PCET from reductively quenched photocatalyst state, K-PHI(e<sup>-</sup>/H<sup>+</sup>), allows employing less oxidative (those having less positive reduction potential) electron acceptors, such as nitrobenzene and diphenyldisulfide in addition to O<sub>2</sub>, to complete the photocatalytic cycle.

Hereby, we demonstrate the employment of K-PHI photocatalyst in C–H amination of electron-rich aromatic hydrocarbons in the synthesis of anilines, and N-arylpyrazoles (Figure 1b).

## Results and Discussion

In the initial catalytic experiment design, 1,3-dimethoxybenzene **1b** has been selected as the substrate and nitrobenzene as the electron acceptor in CH<sub>3</sub>CN. The reaction was investigated under blue light irradiation, using NH<sub>4</sub>OH, as a convenient,

cheap and more atom efficient source of ammonia compared to reported earlier ammonium carbamate.<sup>[12d,17]</sup> Although dichloroethane (DCE) and DMSO were reported in literature as optimal solvents for other photocatalytic systems,<sup>[12d,17]</sup> in these media we obtained **2b** with only 2 and 9% yield respectively (Table 1, entry 1–2). CH<sub>3</sub>CN was found to be the optimal solvent, in which we obtained **2b** with 42% yield along with the recovery of the starting compound (entry 3).

Control experiments without K-PHI, and without electron acceptor further confirmed that this methodology does rely on photocatalyst and excitation with light (entry 4–5). Under aerobic conditions we did not obtain **2b** (entry 6), which is likely due to subsequent oxidation of this compound mediated by O<sub>2</sub>. Using dibenzyl disulfide instead of PhNO<sub>2</sub> gave **2b** with 34% yield (entry 7). 4-nitrotoluene instead of PhNO<sub>2</sub> in CH<sub>3</sub>CN gave **2b** with comparable yield, 43% (Table S3, entry 2). mpg-CN, a carbon nitride material that is capable to store significantly smaller amount of charges,<sup>[28]</sup> did not give **2b** (entry 8). This fact underlines importance of long-lived reductively quenched state of the photocatalyst, such as K-PHI(e<sup>-</sup>/H<sup>+</sup>), during the photocatalyst turn over step. Na-PHI, a carbon nitride material structurally similar to K-PHI,<sup>[19]</sup> which is also able to undergo photocharging,<sup>[29]</sup> gave **2b** in 19% yield (entry 9) likely due to slightly wider optical band gap of 2.78 eV.<sup>[30,31]</sup> Ru- and Ir-polypyridyl complexes did not give **2b** (entry 10, 11), and neither Eosin Y (Entry 12). Taking into account the proposed mechanism (see below),<sup>[12d,17]</sup> these results are explained by the excited state of the tested organic dyes to be not sufficiently oxidative, +0.31... +1.20 V vs. SCE,<sup>[32,33,14]</sup> to produce the radical cation from 1,3-dimethoxybenzene (*E*<sub>1/2</sub> + 1.50 V vs. SCE)<sup>[34]</sup> upon 1-electron oxidation. Apparent quantum yield (AQY) of **2b** mediated by K-PHI is only 0.1% (Figure S3), which underlines that the investigated reaction is indeed challenging.

**Table 1.** Reaction screening and optimization.

Entry	Deviations from Method A <sup>[a]</sup>	Yield [%]
1	DCE (instead of CH <sub>3</sub> CN)	2 (2)
2	DMSO (instead of CH <sub>3</sub> CN)	9 (9)
3	None	42 (42)
4	No photocatalyst	(/)
5	No PhNO <sub>2</sub>	2 (2)
6	O <sub>2</sub> atmosphere (instead of PhNO <sub>2</sub> )	(/)
7	Diphenyl disulphide (instead of PhNO <sub>2</sub> )	34 (34)
8	mpg-CN (10 mg mL <sup>-1</sup> )	(/)
9	Na-PHI (10 mg mL <sup>-1</sup> )	19 (19)
10	[Ru(bpy) <sub>3</sub> ]Cl <sub>2</sub> (2.5% mol)	(/)
11	Ir(ppy) <sub>3</sub> (2.5% mol)	Traces (/)
12	Eosin Y (2.5% mol)	(/)

[a] Reaction conditions (Method A): CH<sub>3</sub>CN (0.5 mL), **1b** (0.04 mmol), PhNO<sub>2</sub> (0.04 mmol), NH<sub>4</sub>OH (0.2 mL, 25% aqueous solution), blue light (465 nm, 50 mW cm<sup>-2</sup>), Ar atmosphere, 30 °C, 24 hours. Conversion is reported in parentheses.

Indeed, quantum efficiencies in photoredox catalysis, both homogeneous and heterogeneous versions, are usually low.<sup>[35]</sup> Nonetheless, this does not represent a bottleneck since low AQY values are compensated by the synthesis of highly valuable active pharmaceutical ingredients (APIs), which is the scope of the developed methodologies in this work. While using K-PHI as the optimal photocatalyst, employment of different ammonia sources (Table S6), wavelength of light (Table S5), solvent (Table S4) did not improve the yield.

Using the optimal conditions (Method A), 1,3,5-trimethoxybenzene **1c** was converted into aniline **2c** with 30% yield (Figure 2). Based on the results of other substrates screening (Figure S10), it has emerged that only compounds bearing highly electron donating groups and characterized by the oxidation potential  $E_{1/2} < 1.5$  V vs. SCE are compatible with the method A.

Despite being weaker nucleophile, pyrazole is coupled with electron rich hydrocarbons **1a–c** with 25, 12 and 59% yield. In this case, however, we conducted the reaction in DCE and used stronger electron acceptor,  $O_2$ , instead of  $PhNO_2$  (Method B).

Taking into account earlier publications and our own findings,<sup>[12d,17]</sup> the proposed mechanism is shown in Figure 3. K-PHI is brought from the ground state to the excited state upon blue photon absorption. Due to the potential of K-PHI valence band, +1.88 V vs. SCE, being more positive than the oxidation potential ( $E_{1/2}$  vs SCE) of hydrocarbons studied in this work, (+1.49 V for 1,3,5-trimethoxybenzene,<sup>[36]</sup> +1.50 V for 1,3-dimethoxybenzene, and +1.81 V for anisole)<sup>[34,36]</sup> the photoinduced electron transfer (PET) is downhill, which produces the contact radical ion pair **1-i**. Nucleophilic attack of ammonia or azole at the surface-bound radical cation gives an intermediate **1-ii**. The importance of the interaction between the radical cation and the surface of heterogeneous photocatalyst is supported by the fact that in case of using K-PHI and *h*BCN,<sup>[17]</sup> additional mediator is not required, while amination of electron rich aromatic

hydrocarbons with azoles requires TEMPO as the additive.<sup>[12d]</sup> The product **2** is formed upon **1-ii** decomposition *via* PCET to an electron acceptor. The catalytic cycle is closed. Microporous structure of K-PHI can accommodate up to 1 mmol of electrons and charge compensating protons per 1 gram of the material.<sup>[22,26,37]</sup> Although photocharged state, K-PHI( $e^-$ ), is a persistent radical under anaerobic conditions, in the studied reaction, it is only a transient specie –  $O_2$  or  $PhNO_2$  are reduced by K-PHI( $e^-$ ) to  $H_2O_2$  or  $Ph-N=N-Ph$  (and  $PhNH_2$ ) respectively.<sup>[26]</sup>

Given that the conduction band potential in K-PHI is only  $-0.82$  V vs. SCE, PET to  $PhNO_2$  ( $E_{1/2} = -1.19$  V vs. SCE) is uphill.<sup>[34]</sup> However, reduction of  $PhNO_2$  to the corresponding radical upon  $e^-/H^+$  transfer is downhill ( $E_{1/2} = -0.404$  V vs. SCE).<sup>[38]</sup> More specifically, reduction of  $PhNO_2$  *via* MS-PCET is by  $75$   $kJ\ mol^{-1}$  more favorable compared to PET (Table S11). Although reduction of  $O_2$  to the superoxide radical *via* PET is downhill, MS-PCET makes this process by  $25$   $kJ\ mol^{-1}$  more facile and according to Marcus theory faster.<sup>[39]</sup> This fact is likely to explain that in order to employ pyrazole (weaker nucleophile compared to  $NH_3$ ), stronger electron acceptor ( $O_2$ ) is required so that the decomposition of the contact radical ion pair **1-ii** with the formation of the product **2** proceeds faster than the back transfer of electron (and proton). Methyl viologen, a one-electron oxidant, despite having reduction potential ( $E_{1/2} = -0.69$  V vs. SCE)<sup>[40]</sup> more positive than the potential of K-PHI conduction band, does not enable hydrocarbons amination (Table S3, entry 4,5). However, diphenyldisulfide does enable the reaction (Table 1, entry 7) due to the fact that it serves as H-atom acceptor – it is reduced to thiophenol. Importance of temporary electron storage in carbon nitride photocatalyst is once again supported by the fact that Na-PHI gives a coupling product (Table 1, entry 9). Except PHI that is characterized by strongly positive potential of the valence band and ionic structure no other photocatalytic system studied in this work enables the reaction. Combination of these properties in one

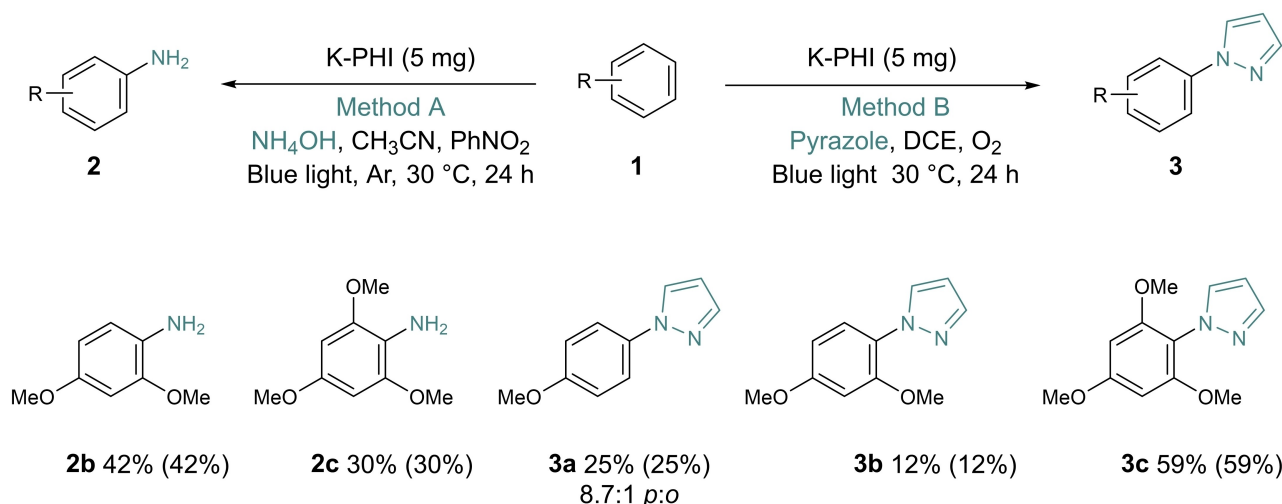


**Figure 2.** Reaction scope. Reaction conditions for Method A: K-PHI (5 mg),  $CH_3CN$  (0.5 mL), substrate **1** (1 eq., 0.3–0.5 mmol), nitrobenzene (1 equiv.),  $NH_4OH$  (0.2 mL, 25% aqueous solution), blue light (465 nm,  $50$   $mW\ cm^{-2}$ , Ar atmosphere,  $30$  °C, 24 hours). Reaction conditions for Method B: K-PHI (5 mg), DCE (0.5 mL), substrate **1** (1 equiv., 0.3–0.5 mmol), pyrazole (4 equiv.), blue light (465 nm,  $50$   $mW\ cm^{-2}$ ),  $O_2$  atmosphere,  $30$  °C, 24 hours. Conversion is reported in parentheses. Yields and conversions were determined by GC-MS. More details about experimental procedures are provided in the Supporting Information.

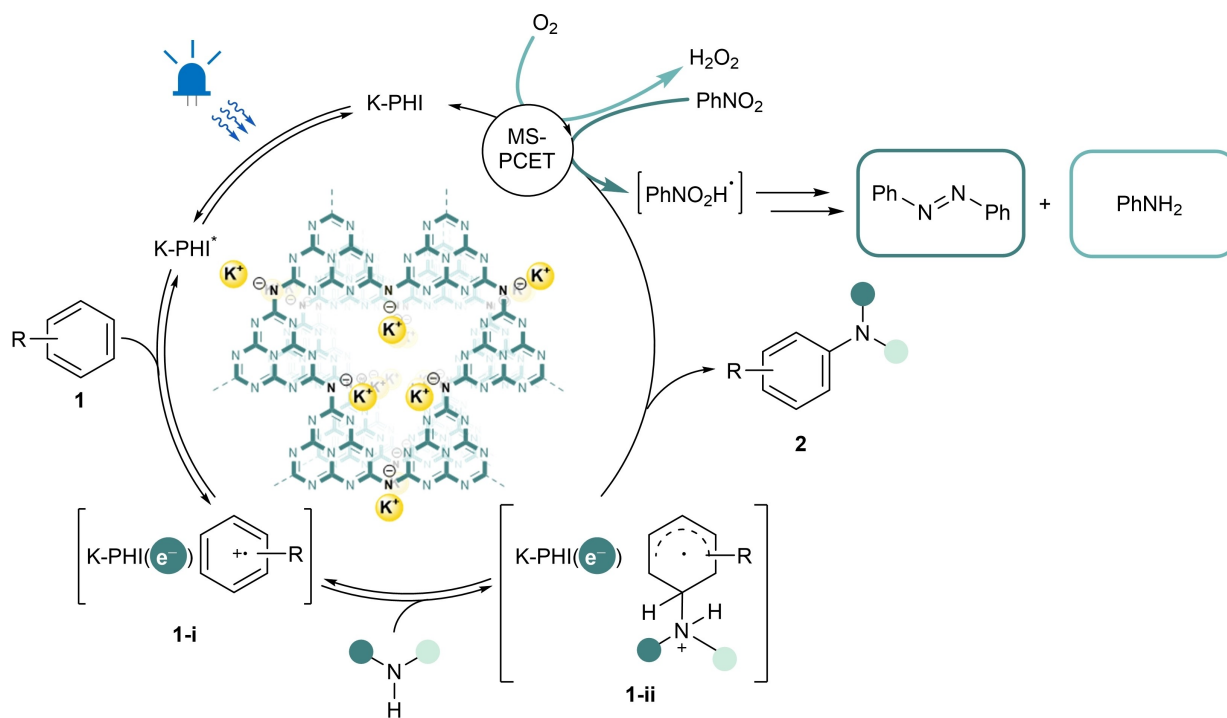


Figure 3. Reaction mechanism.

nanomaterial makes it active in amination of aromatic hydrocarbons. Thus, strongly positive potential of the valence band facilitates formation of the radical cation upon photoinduced electron transfer. Ionic structure stabilizes negative charge, while the negatively charged surface of PHI serves as a counterion in the tentative intermediate 1-i.

## Conclusion

A methodology for C–H amination of aromatic hydrocarbon has been developed using K-PHI as a photocatalyst. Owing to a highly positive valence band potential (+1.88 V vs. SCE), it is able to oxidize substituted benzenes characterized by the oxidation potentials ranging from +1.49 to +1.81 V vs. SCE. The generated open-shell intermediates gain increased reactivity towards *N*-nucleophiles, namely ammonia and pyrazole. With this strategy, 5 examples of C–N coupling products have been prepared with 12–59% yield. Due to K-PHI property to store multiple electrons in the microporous structure of the material, a complementary process – reduction of electron acceptors becomes thermodynamically more feasible. This fact is likely to explain that the coupling of hydrocarbons with ammonia proceeds in the presence of nitrobenzene, while less nucleophilic pyrazoles require stronger oxidant – O<sub>2</sub>. Such observation underlines importance of proper selection of electron (and proton) acceptors in semiconductor photocatalysis, which could lower the energy barriers and to improve the rate and reactions efficacy. Concluding, by employing the state-of-the-art organic semiconductor photocatalyst, K-PHI, it is

possible to avoid the use of transition metals in C–H amination. Further reactions from our lab employing PCET from/to carbon nitride photocatalysts will be reported.

## Experimental Section

**K-PHI synthesis.**<sup>[21]</sup> A mixture of lithium chloride (3.71 g), potassium chloride (4.54 g), and 5-aminotetrazole (1.65 g) was ground in ball mill for 5 min at the shaking rate 25 s<sup>-1</sup>. Reaction mixture was transferred into a porcelain crucible and covered with a lid. A crucible was placed in the oven and heated under constant nitrogen flow (15 Lmin<sup>-1</sup>) and atmospheric pressure at the following temperature regime: heating from room temperature to 600 °C for 4 hours, annealing at 600 °C for 4 hours. After completion of the heating program, the crucible was allowed to cool slowly to room temperature under nitrogen flow. The crude product was removed from the crucible, washed with deionized water (100 mL) for 3 hours in order to remove salts, then filtered, extensively washed with deionized water, and dried in a vacuum oven (20 mbar) at 50 °C for 15 h.

**Method A.** K-PHI (5 mg), acetonitrile (0.5 mL), a substrate **1** (1 equiv., 0.05 mmol of **1a**, 0.04 mmol of **1b** or 0.03 mmol of **1c**), nitrobenzene (1 equiv.), and NH<sub>4</sub>OH (0.2 mL, 25% aqueous solution) were mixed in a vial. The mixture was purged with Ar and closed with a cap. The reaction mixture was stirred under blue light irradiation (465 nm, 50 mWcm<sup>-2</sup>), at 30 °C for 24 h. After the irradiation, the catalyst was separated by centrifugation. CHCl<sub>3</sub> (3.5 mL) and water (0.3 mL) were added to the reaction mixture. The layers were separated and the organic layer was dried under NaSO<sub>4</sub>. The clear solution was analyzed by GC-MS.

**Method B.** K-PHI (5 mg), DCE (0.5 mL), substrate **1** (1 equiv., 0.05 mmol of **1a**, 0.04 mmol of **1b** or 0.03 mmol of **1c**) and

pyrazole (4 eq.) were mixed in a vial. The mixture was filled with O<sub>2</sub> and closed with a cap. The reaction mixture was stirred under blue light irradiation (465 nm, 50 mWcm<sup>-2</sup>) at 30 °C for 24 hours. After the irradiation, the catalyst was separated by centrifugation and the reaction mixture was analyzed by GC-MS.

## Acknowledgements

The authors gratefully acknowledge European Commission (DEC-ADE, grant agreement ID: 862030) and Max Planck Society for providing financial support for this project and Katharina ten Brummelhuis. Open Access funding enabled and organized by Projekt DEAL.

## Conflict of Interest

A patent WO/2019/081036 has been filed by Max Planck Gesellschaft zur Förderung der Wissenschaften E.V. in which O.S. is listed as the co-author.

## Data Availability Statement

The data that support the findings of this study are available from the corresponding author upon reasonable request.

**Keywords:** Amination · Carbon nitride · C–N coupling · PCET · Photocatalysis

- [1] a) D. Schultz, L. C. Campeau, *Nat. Chem.* **2020**, *12*, 661–664; b) D. C. Blakemore, L. Castro, I. Churcher, D. C. Rees, A. W. Thomas, D. M. Wilson, A. Wood, *Nat. Chem.* **2018**, *10*, 383–394.
- [2] D. W. C. MacMillan, *Nature* **2008**, *455*, 304–308.
- [3] Y. Kawamata, P. S. Baran, *Joule* **2020**, *4*, 701–704.
- [4] S. Wu, J. Žurauskas, M. Domański, P. S. Hitzfeld, V. Butera, D. J. Scott, J. Rehbein, A. Kumar, E. Thyryhaug, J. Hauer, J. P. Barham, *Org. Chem. Front.* **2021**, *8*, 1132–1142.
- [5] S. Wu, J. Kaur, T. A. Karl, X. Tian, J. P. Barham, *Angew. Chem. Int. Ed.* **2022**, *61*, e202107811.
- [6] D. A. N. a. D. W. C. MacMillan, *Science* **2008**, *322*, 77–80.
- [7] L. Candish, K. D. Collins, G. C. Cook, J. J. Douglas, A. Gómez-Suárez, A. Jolitt, S. Keese, *Chem. Rev.* **2022**, *122*, 2907–2980.
- [8] R. C. McAtee, E. J. McClain, C. R. J. Stephenson, *Trends Chem.* **2019**, *1*, 111–125.
- [9] a) L. Li, J.-Z. Li, Y.-B. Sun, C.-M. Luo, H. Qiu, K. Tang, H. Liu, W.-T. Wei, *Org. Lett.* **2022**, *24*, 4704–4709; b) X.-C. Yu, C.-C. Zhang, L.-T. Wang, J.-Z. Li, T. Li, W.-T. Wei, *Org. Chem. Front.* **2022**, *9*, 4757–4781.
- [10] J. Boström, D. G. Brown, R. J. Young, G. M. Keserü, *Nat. Rev. Drug Discovery* **2018**, *17*, 709–727.
- [11] a) Y.-N. Zheng, H. Zheng, T. Li, W.-T. Wei, *ChemSusChem* **2021**, *14*, 5340–5358; b) H.-Z. Wang, J.-Z. Li, Z. Guo, H. Zheng, W.-T. Wei, *ChemSusChem* **2021**, *14*, 4658–4670.
- [12] a) Y. Zhao, B. Huang, C. Yang, B. Li, B. Gou, W. Xia, *ACS Catal.* **2017**, *7*, 2446–2451; b) C. Rosso, S. Gisbertz, J. D. Williams, H. P. L. Gemoets, W. Debrouwer, B. Pieber, C. O. Kappe, *React. Chem. Eng.* **2020**, *5*, 597–604; c) E. B. Corcoran, J. P. McMullen, F. Levesque, M. K. Wismer, J. R. Naber, *Angew. Chem. Int. Ed. Engl.* **2020**, *59*, 11964–11968; d) A. Romero Nathan, A. Margrey Kaila, E. Tay Nicholas, A. Nicewicz David, *Science* **2015**, *349*, 1326–1330.
- [13] E. B. Corcoran, M. T. Pirnot, S. Lin, S. D. Dreher, D. A. DiRocco, I. W. Davies, S. L. Buchwald, D. W. C. MacMillan, *Science* **2016**, *353*, 279–283.
- [14] I. Ghosh, J. Khamrai, A. Savateev, N. Shlapakov, M. Antonietti, B. König, *Science* **2019**, *365*, 360–366.
- [15] S. Gisbertz, S. Reischauer, B. Pieber, *Nat. Catal.* **2020**, *3*, 611–620.
- [16] A. Vijeta, C. Casadevall, E. Reisner, *Angew. Chem. Int. Ed.* **2022**, *61*, e202203176.
- [17] M. Zheng, I. Ghosh, B. König, X. Wang, *ChemCatChem* **2019**, *11*, 703–706.
- [18] Y. Markushyna, C. A. Smith, A. Savateev, *Eur. J. Org. Chem.* **2020**, 1294–1309.
- [19] Z. Chen, A. Savateev, S. Pronkin, V. Papaefthimiou, C. Wolff, M. G. Willinger, E. Willinger, D. Neher, M. Antonietti, D. Dontsova, *Adv. Mater.* **2017**, *29*, 1700555.
- [20] A. Savateev, M. Antonietti, *ChemCatChem* **2019**, *11*, 6166–6176.
- [21] A. Savateev, N. V. Tarakina, V. Strauss, T. Hussain, K. ten Brummelhuis, J. M. Sánchez Vadillo, Y. Markushyna, S. Mazzanti, A. P. Tyutyunnik, R. Walczak, M. Oschatz, D. M. Guldi, A. Karton, M. Antonietti, *Angew. Chem. Int. Ed. Engl.* **2020**, *59*, 15061–15068.
- [22] O. Savateev, *Adv. Energy Mater.* **2022**, *12*, 2200352.
- [23] F. Podjaski, B. V. Lotsch, *Adv. Energy Mater.* **2021**, *11*, 2003049.
- [24] S. Mazzanti, A. Savateev, *ChemPlusChem* **2020**, *85*, 2499–2517.
- [25] H. Schlöberg, J. Kröger, G. Savasci, M. W. Terban, S. Bette, I. Moudrakovski, V. Duppel, F. Podjaski, R. Siegel, J. Senker, R. E. Dinnebier, C. Ochsenfeld, B. V. Lotsch, *Chem. Mater.* **2019**, *31*, 7478–7486.
- [26] S. Mazzanti, C. Schmitt, K. ten Brummelhuis, M. Antonietti, A. Savateev, *Exploration* **2021**, *1*, 20210063.
- [27] V. W. Lau, D. Klose, H. Kasap, F. Podjaski, M. C. Pignie, E. Reisner, G. Jeschke, B. V. Lotsch, *Angew. Chem. Int. Ed. Engl.* **2017**, *56*, 510–514.
- [28] Y. Markushyna, P. Lamagni, C. Teutloff, J. Catalano, N. Lock, G. Zhang, M. Antonietti, A. Savateev, *J. Mater. Chem. A* **2019**, *7*, 24771–24775.
- [29] J. Kröger, F. Podjaski, G. Savasci, I. Moudrakovski, A. Jiménez-Solano, M. W. Terban, S. Bette, V. Duppel, M. Joos, A. Senocrate, R. Dinnebier, C. Ochsenfeld, B. V. Lotsch, *Adv. Mater.* **2022**, *34*, 2107061.
- [30] I. F. Teixeira, N. V. Tarakina, I. F. Silva, G. A. Atta Diab, N. L. Salas, A. Savateev, M. Antonietti, *J. Mater. Chem. A* **2022**, *10*, 18156–18161.
- [31] I. F. Teixeira, N. V. Tarakina, I. F. Silva, N. López-Salas, A. Savateev, M. Antonietti, *Adv. Sustainable Syst.* **2022**, *6*, 2100429.
- [32] T. Koike, M. Akita, *Inorg. Chem. Front.* **2014**, *1*, 562–576.
- [33] V. Srivastava, P. P. Singh, *RSC Adv.* **2017**, *7*, 31377–31392.
- [34] H. G. Roth, N. A. Romero, D. A. Nicewicz, *Synlett* **2016**, *27*, 714–723.
- [35] Q. Liu, H. Cao, W. Xu, J. Li, Q. Zhou, W. Tao, H. Zhu, X. Cao, L. Zhong, J. Lu, X. Peng, J. Wu, *Cell Rep. Phys. Sci.* **2021**, *2*, 100491.
- [36] N. L. Weinberg, H. R. Weinberg, *Chem. Rev.* **1968**, *68*, 449–523.
- [37] a) H. Ou, C. Tang, X. Chen, M. Zhou, X. Wang, *ACS Catal.* **2019**, *9*, 2949–2955; b) A. Savateev, B. Kurpil, A. Mishchenko, G. Zhang, M. Antonietti, *Chem. Sci.* **2018**, *9*, 3584–3591; c) F. Podjaski, J. Kroger, B. V. Lotsch, *Adv. Mater.* **2018**, *30*, 1705477.
- [38] S. C. Jensen, S. Bettis Homan, E. A. Weiss, *J. Am. Chem. Soc.* **2016**, *138*, 1591–1600.
- [39] R. A. Marcus, *Angew. Chem. Int. Ed. Engl.* **1993**, *32*, 1111–1121.
- [40] M. D. Ward, J. R. White, A. J. Bard, *J. Am. Chem. Soc.* **1983**, *105*, 27–31.

Manuscript received: November 9, 2022

Revised manuscript received: January 4, 2023

Accepted manuscript online: January 13, 2023

Version of record online: January 31, 2023